

# Engineering Notes

## Recursive Least Squares for Online Dynamic Identification on Gas Turbine Engines

Zhuo Li,\* Theoklis Nikolaidis,† and Devaiah Nalianda†  
*Cranfield University,  
 Cranfield, England MK43 0AL, United Kingdom*

DOI: 10.2514/1.G000408

### I. Introduction

ONLINE identification for a gas turbine engine is vital for health monitoring and control decisions because the engine electronic control system uses the identified model to analyze the performance for optimization of fuel consumption, a response to the pilot command, as well as engine life protection. Since a gas turbine engine is a complex system and operating at variant working conditions, it behaves nonlinearly through different power transition levels and at different operating points. An adaptive approach is required to capture the dynamics of its performance.

Dynamic identification for gas turbine engines is mostly carried by frequency analysis through the experiments with sinusoidal fuel input. From the research by Evans et al. [1], different frequency responses are shown at different operating points [1]. A set of estimated functions is used for representation over the full operating range. For the process of simplification, an adaptive approach needs to be implemented so that the estimated model can be evolved along with the change of engine dynamics.

Isermann et al. [2] compared six methods commonly used in the industry, and most of the online methods were based on the theory of least squares and likelihood [2]. These methods are particularly favored to the online identification because of their simplicity and computing efficiency. They did not require iterations and training like neural networks, but the accuracy of these methods was sometimes compromised.

The recursive least squares (RLS) algorithm is well known for tracking dynamic systems. Torres et al. [3] attempted to identify the dynamic of the gas turbine engine offline, mainly at steady states with stochastic signals. Arkov et al. [4] focused on real-time identification for transient operations and concluded that an engine system could be averaged to a time-invariant first- or second-order transfer function by the extended RLS [4]. The tracking speed and accuracy for the RLS could be improved with a different design of forgetting factors. The effect of using a forgetting factor was to shift the estimating average toward the most recent data, such as that in the work by Paleologu et al. [5]. In this paper, classic and modified RLS

algorithms [directional forgetting RLS (RLS-DF), RLS with a constant stabilizing factor (RLS-SI), and RLS with a varying stabilizing factor (RLS-SV)] were investigated for online dynamic identification of gas turbine engines. The RLS methods were evaluated for their self-adaptive capabilities, as well as their reliability on steady states and transient dynamics.

The verification of these algorithms is conducted through the identification process on a simulated gas turbine engine. The engine model is developed to a component level by using the inter-component volume (ICV) method with variable gas properties in order to obtain an accurate performance estimation as close as possible to the real engine. The validation of these methods is applied by taking the comparison of the estimated results to the outputs of the engine model. All tested RLS algorithms are constructed in parallel with the engine model, and an attempt is made to identify the non-parametric models from a reading of the engine's inputs and outputs. A schematic sketch is shown in Fig. 1.

### II. Gas Turbine Engine Model

The inter-component volume method models the engine from intake to nozzle [6]. The model is constructed of mechanical and turbomachinery subsystems. The gas enthalpy, entropy, and general properties in the subsystems are estimated from either component characteristics or tables, or through an iterative process [7]. The variable gas properties are determined from the prediction of moisture caloric properties [8]. The volume constructed between components provides damping effects to simulate gas propagation through the chamber of its upstream component [9]. The change of fuel flow controls the thermodynamics in the combustor, which breaks the energy balance between compressors and turbines. The transient performance of the engine is created by the imbalance of compressor and turbine power. The energy disturbance is located in the middle of the engine and transferred sequentially from high- to lower-pressure components. Finally, the imbalanced power results in the change of shaft speed. The volume dynamics of turbomachinery components are estimated through partial derivative equations, previously demonstrated by Kulikov and Thompson [10].

### III. Recursive Least-Squares Identification Techniques

A gas turbine engine is a nonlinear system. The nonlinearity is contributed to by the iteration and mapping process from component maps, as well as the variable gas properties in the ICV model. The engine performance can be linearized if the sampling time is selected sufficiently small so that the dynamic behavior within each time interval  $k$  can be assumed as linear time invariant (LTI). Therefore, the entire transient performance is superposed by an individual LTI system from each sampling time. Each LTI can be expressed in a discrete format as

$$X(k+1) = AX(k) + BU(k) \quad (1)$$

where  $A$  and  $B$  are coefficient matrices.

The selection of state variables must be sufficient to describe the dynamics of the interested engine parameters [11]. The parameters that are observable and controllable can be included in the state matrix  $X$  of Eq. (1). For control purposes, the relative shaft speed or compressor/engine pressure ratio is commonly used as a state variable. The dynamics of other parameters, such as specific fuel consumption and turbine entry temperature, are sometimes chosen to be identified for ensuring fuel economy and life protection. The fuel flow  $w_{ff}$  is commonly chosen as the control input  $u$  for gas turbine engines. As a result, the number of state variables  $n$  in Eq. (2) depends

\*Ph.D. Student, Propulsion Engineering Centre, School of Aerospace Transport and Manufacturing.

†Lecturer, Propulsion Engineering Centre, School of Aerospace Transport and Manufacturing.

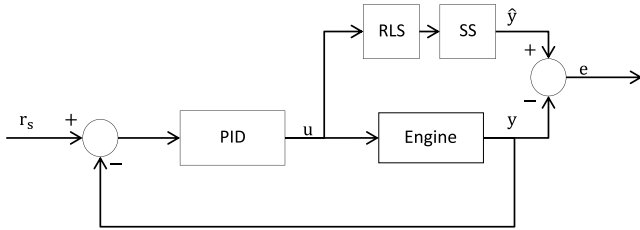


**Fig. 1** Constructed RLS algorithms in parallel with the closed-loop engine system (PID, proportional-integral-derivative; RLS, recursive least squares; and SS, state space model).

on the number of interested engine parameters and their associated parameters that affect the dynamic of these interested parameters. For example, developing a dynamic model of a low-pressure shaft from a twin-spool engine requires including the relative speed of the low-pressure shaft as well as the speed of the high-pressure shaft, because their dynamic performances are related. Therefore, Eq. (1) can be written as

$$\begin{bmatrix} x_1(k+1) \\ \vdots \\ x_n(k+1) \end{bmatrix} = \begin{bmatrix} a_{11} & \cdots & a_{1n} \\ \vdots & \ddots & \vdots \\ a_{n1} & \cdots & a_{nn} \end{bmatrix} \begin{bmatrix} x_1(k) \\ \vdots \\ x_n(k) \end{bmatrix} + \begin{bmatrix} b_1 \\ \vdots \\ b_n \end{bmatrix} u(k) \quad (2)$$

The values of the elements in matrices  $A$  and  $B$  in Eq. (2) are unknown and required to be identified by the RLS algorithms.

### A. Recursive Least Squares

The recursive least-squares algorithm is an extension from the least squares (LS). The RLS convolutes the dynamics of the parameters to the covariance matrix instead of storing all the data to the matrix in the LS [12]. This removes the infinitive expansion of the matrix size in the LS as time passes on, and it allows online identification when possible.

The self-adaptive capability allowing the estimation can be updated at each sampling time from new available data. The error is taken between the new engine data  $y(k)$  and the estimated state value  $\hat{y}(k)$  with the system noise  $n(k)$  in Eq. (3). The noise can be excluded due to the implementation of the ICV model. We have

$$\varepsilon(k) = y(k) - n(k) - \hat{y}(k) = y(k) - n(k) - \varphi(k)^T \theta(k-1) \quad (3)$$

The parametric matrix  $\varphi$  is combined with measurement of the input and states:

$$\varphi(k) = [X(k), u(k)]^T \quad (4)$$

The value of the objective parameter  $\theta$  from the previous time step is

$$\theta(k-1) = [A^T(k-1), B^T(k-1)]^T \quad (5)$$

The covariance matrix  $P$  is

$$P(k) = \left[ \begin{bmatrix} \varphi(0) \\ \vdots \\ \varphi(k-1) \end{bmatrix}^T \begin{bmatrix} \varphi(0) \\ \vdots \\ \varphi(k-1) \end{bmatrix} \right]^{-1} \quad (6)$$

The covariance matrix can be estimated by using the matrix inversion lemma. This method saves computing memory and eliminates operation of the matrix inversion; see Eq. (6) [12]. The update of the covariance matrix becomes

$$P(k+1) = P(k) \left[ I - \frac{\varphi(k)\varphi^T(k)P(k)}{1 + \varphi^T(k)P(k)\varphi(k)} \right] \quad (7)$$

and the updated estimations of  $A$  and  $B$  are

$$\theta(k+1) = \theta(k) + P(k+1)\varphi(k)\varepsilon(k) \quad (8)$$

The main advantage of RLS over LS is simplicity and efficiency. The updated estimations of  $A$  and  $B$  only require data from one step backward. The existing stochastic noise with zero mean from the engine outputs consistently excites the engine parameters when the engine is operating near steady states. Such white noise ensures the parameter's observability or ensures full rank of the covariance matrix [12]. The tracking performance can be improved by introducing forgetting factors so that the estimation can be shifted to the latest data, allowing the RLS to be adaptive of both the transient and steady states.

### B. RLS with Forgetting Factors

The RLS algorithm with implementation of the constant forgetting factor requires a modified covariance matrix:

$$P(k+1) = \lambda^{-1}P(k) \left[ I - \frac{\varphi(k)\varphi^T(k)P(k)}{\lambda + \varphi^T(k)P(k)\varphi(k)} \right] \quad (9)$$

The value of  $\lambda$  is selected between 0.9 and 1.0 for a fixed forgetting process. The forgetting factor controls the dumping rate to the old data. If unity is selected, the algorithm is the same as the RLS, which accumulates all past data. Recent research has focused on improving the converging speed to the real system. A robust variable forgetting factor to the RLS was introduced by Paleologu et al. [5]. The selection of forgetting factors [Eq. (10)] is controlled by the error  $\varepsilon$ , which is the difference between the measurement and its estimation, i.e.,

$$\lambda = \min \left\{ \frac{\sigma_e(k)\sigma_v(k)}{\zeta + |\sigma_e(k) - \sigma_v(k)|}, \lambda_{\max} \right\} \quad (10)$$

where  $\sigma_e$  and  $\sigma_v$  are the functions describing the square of the error, and they control the power of correction at each sampling time step. However, when the error  $\varepsilon$  tends toward zero, the values of  $\sigma_e$  and  $\sigma_v$  approach zero. The minimum value of  $\lambda$  can be as close as zero in Eq. (10), which is most likely to happen near steady states. As a result, the absolute values of the elements in the covariance matrix in Eq. (9) can be increased exponentially to infinity. However, the values are expected to approach a constant value when operating in a steady state. The value of the forgetting factor  $\lambda$  in Eq. (9) of less than one increases the covariance trace over time if the engine outputs are a lack excitation [12], and the inverse  $\lambda$  causes the divergence of the covariance matrix.

A directional forgetting algorithm (RLS-DF) is designed to avoid covariance windup by removing the multiplication of the inverse forgetting factor from Eq. (9) to Eq. (11) [12]:

$$P(k+1) = P(k) \left[ I - \frac{\varphi(k)\varphi^T(k)P(k)}{\lambda^{-1}(k) + \varphi^T(k)P(k)\varphi(k)} \right] \quad (11)$$

The value of the variable forgetting factor is determined by the direction in parameter space, which is to the direction of vector  $\varphi$  [12]. The direction forgetting factor is selected as

$$\lambda(k+1) = r - \frac{1-r}{\varphi^T(k)P(k)\varphi(k)} \quad (12)$$

where  $r$  acts as a fixed forgetting factor, which controls the tracking speed to the engine performance. The value of  $r$  is suggested to be between zero and one.

### C. Stabilized RLS Algorithms

For time-variant systems such as gas turbine engines, the covariance matrix must not be asymptotically singular. The method suggested by Milek and Kraus stabilized the estimation process in the RLS by introducing the stabilizing invariant factors (RLS-SI) or variable factors (RLS-SV) [13,14]. The modification on the covariance with the linear forgetting algorithm becomes

$$P(k+1) = \mu \hat{P}(k+1) + gI \quad (13)$$

$\hat{P}(k+1)$  in Eq. (13) is normalized as  $P(k+1)$  in Eq. (11).  $I$  is an identity matrix. The additional term added to the end of Eq. (13) is the adjustable matrix, which damps the growth on the value of the covariance matrix. The constrained covariance matrix stabilizes the change on the value of elements in the coefficient matrix in Eq. (2).

The modification of the covariance matrix can lead the value to diverge if the estimator is not persistently excited. Therefore, the eigenvalues  $\lambda$  of the covariance matrix must be bounded, and they cannot be less than zero:

$$0 < \lambda_{\min} < \lambda < \lambda_{\max} \quad (14)$$

The value of the eigenvalue can be calculated as

$$\lambda(k+1) = \mu\lambda(k) - \frac{\lambda(k)|\varphi(k)|^2}{1 + |\varphi(k)|^2} + g \quad (15)$$

The engine parameter matrix has been normalized to  $\hat{\varphi}(k)$ , i.e.,

$$\hat{\varphi}(k) = \varphi(k)/|\varphi(k)| \quad (16)$$

The normalized value of parameter matrix  $\hat{\varphi}(k)$  and the normalized covariance  $\hat{P}(k+1)$  are obtained by iterations from an initial estimation of the covariance matrix, and the bounded eigenvalues of  $\hat{P}(k+1)$  are checked through Eq. (17). We have

$$\lambda_{\max} = \frac{g}{1-\mu}$$

$$\lambda_{\min} = \frac{\mu + g|\varphi(k)|^2 - 1 + \sqrt{(1-\mu-g|\varphi(k)|^2)^2 + 4g|\varphi(k)|^2(2-\mu)}}{2|\varphi(k)|^2(2-\mu)} \quad (17)$$

where  $0 < \mu < 1$ ,  $\rho > 0$ , and  $g = \mu \cdot \rho$ .

In the RLS-SV, the performance of the RLS-SI is improved by including the adjustable term in Eq. (13). Instead of using a constant forgetting value  $g$  in the RLS-SI, a variable value is determined by signal levels  $\varphi(k)$  from Eq. (18). The procedure of other estimation steps remains the same as the RLS-SI. The variable value is

$$g(k) = \frac{g}{\varphi^T(k)\varphi(k)} \quad (18)$$

#### IV. Simulation Results

A twin-spool turbofan engine was simulated to validate the performance of the aforementioned identification algorithms, and the engine configuration is shown in Fig. 2. The airflow enters from the intake (IN) and through the low-pressure compressor (LPC) to the high-pressure compressor (HPC); is mixed and burned with the fuel flow in the combustor (COMB); then is discharged through the high-pressure turbine (HPT) to the low-pressure turbine (LPT); and, finally, the gas is exhausted from the nozzle. The control of the fuel flow will trigger the transient disturbance from the higher pressure to lower components.

The twin spool turbofan engine has been modelled to operate at design point using on the data shown in Table 1. The transient cycle uses the percentage of corrected speed (PCN) for low-pressure shaft

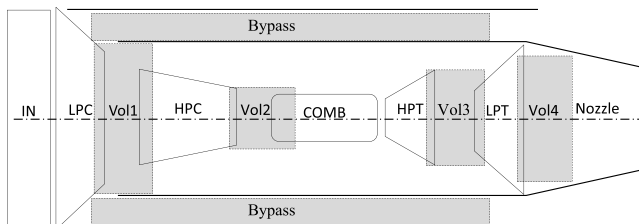


Fig. 2 Modeled two-spool turbofan engine by ICV method; volumes (Vol) are shaded areas.

Table 1 Design point of the two-spool turbofan engine

Parameter	Value	Unit
Ambient condition	ISA SLS	—
Intake mass flow	44.8	kg/s
Low-pressure compressor pressure ratio (LPC PR)	1.70	—
Low-pressure compressor isentropic efficiency	88	%
High-pressure compressor pressure ratio (HPC PR)	5.60	—
High-pressure compressor isentropic efficiency	88	%
Fuel flow	0.2466	kg/s
High-pressure turbine isentropic efficiency	89	%
Low-pressure turbine isentropic efficiency	89	%
Moment of inertia for low-pressure shaft	10	kg/m <sup>2</sup>
Moment of inertia for high-pressure shaft	8.4	kg/m <sup>2</sup>
PCN of low-pressure shaft to 170 RPS	100	%
PCN of high-pressure shaft to 177 RPS	100	%
Volume 1	1.50	m <sup>3</sup>
Volume 2	0.50	m <sup>3</sup>
Volume 3	0.38	m <sup>3</sup>
Volume 4	0.50	m <sup>3</sup>

Note: ISA, international standard atmosphere; SLS, sea level standard.

as the control reference. The transient cycles are performed between 60 and 100% of the corrected speed of the low-pressure shaft, which corresponds to a LPC PR of 1.21 ~ 1.70, a HPC PR of 3.41 ~ 5.31, and a steady-state fuel flow of 0.07 ~ 0.24 kg/s. A volume module is added to the downstream of each turbomachinery component according to the ICV modeling technique.

A closed-loop design was implemented for the engine system. A proportional-integral controller with 0.4 of a proportional gain and 0.2 of an integral gain were added in front of the engine model, as shown in Fig. 1. The value of fuel input was determined by the controller from the difference between the control reference and the engine relative shaft speed.

A state-space (SS) model is connected to the RLS block as shown in Fig. 1, and it is used to reproduce the results of the state variables from the identified model. The state-space model is a linear model. The nonlinearity is obtained by consistently superposing the values in matrices  $A$  and  $B$  from each time step. The performances of algorithms RLS, RLS-DF, RLS-SI, and RLS-SV are compared through the errors between the outputs from their SS models and the engine outputs.

According to Ruano et al., high-pressure components can be approximated to the first order and low-pressure dynamics can be considered second order [15]. The dynamic of the compressor pressure ratio can be estimated by a second-order state-space model:

$$\begin{bmatrix} \text{PR}_{\text{LPC}}(k+1) \\ \text{PR}_{\text{HPC}}(k+1) \end{bmatrix} = A \begin{bmatrix} \text{PR}_{\text{LPC}}(k) \\ \text{PR}_{\text{HPC}}(k) \end{bmatrix} + B W_{\text{ff}}(k) \quad (19)$$

where  $A$  is a  $2 \times 2$  matrix due to two state variables. Fuel flow is the only control variable, so  $B$  is a  $2 \times 1$  matrix.

The values of the collecting factors in the RLS-SV and RLS-SI are chosen to be  $\rho = 0.99$  and  $\mu = 0.99$ ; the forgetting factor for the RLS-DF is  $r = 0.8$ . Furthermore, an identity matrix ( $3 \times 3$ ) is assumed for the covariance matrix in Eq. (17) and an initial value of  $A$  and  $B$  is required to be approximated at the beginning of the simulation. A comparison among the performances of RLS, RLS-DF, RLS-SI, and RLS-SV on the estimation of the compressor pressure ratio to the engine model is shown in Fig. 3. The figure shows that all modified RLS methods are capable of providing accurate approximations to the running line given by the ICV engine model through the entire 225 s with a 0.004 s sampling time. The sampling time is chosen for ensuring the convergence of the iterative processes in the ICV model.

The percentage error on the estimations to the engine outputs in Fig. 4 shows all modified RLS methods drop the tracking accuracy while the engine is operating at transient states. The reduction in accuracy is caused by the delay of model updates and a large gradient change of the operating line during transient operation. The largest estimation errors appear at the beginning of transient operations due to the lack of receding knowledge at the initial estimation.

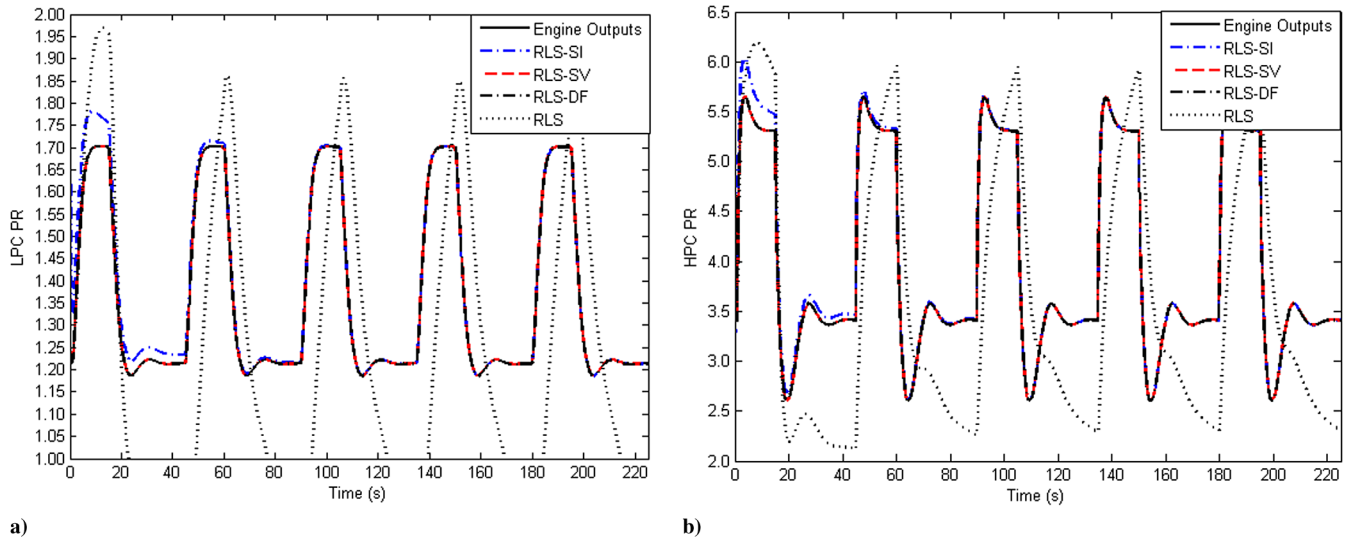


Fig. 3 Comparison of tracking performance on the dynamic of a) LPC PR and b) HPC PR.

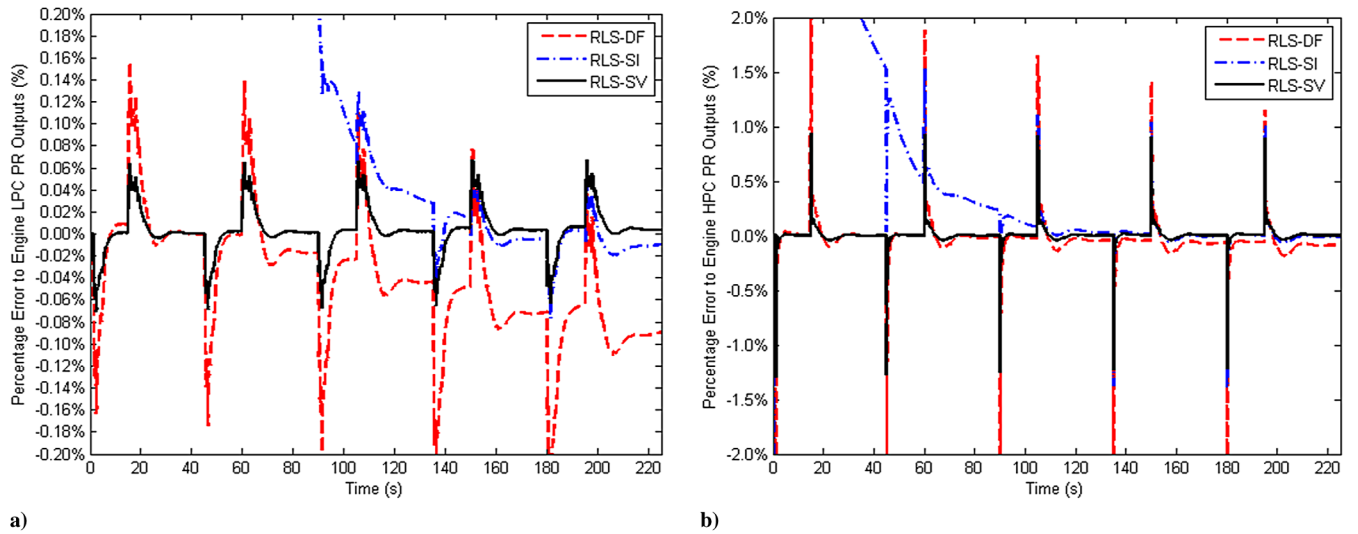


Fig. 4 Percentage error of the estimations from RLS algorithms to the engine: a) LPC PR and b) HPC PR.

The fixed values of collecting factors ( $\mu$  and  $g$ ) in the RLS-SI control the convergent speed of the estimated model to the engine system. Reducing the  $\mu$  value can reduce the recursive power to the normalized covariance matrix in Eq. (13); it also reduces the power of the correcting

term in Eq. (13). Therefore, the mean error [Eq. (20)] is calculated to measure the accuracy of the RLS-SI with a different combination of the values of collecting factors; see Fig. 5. From the results, reducing the value on either factor will result in an increase of the mean error:

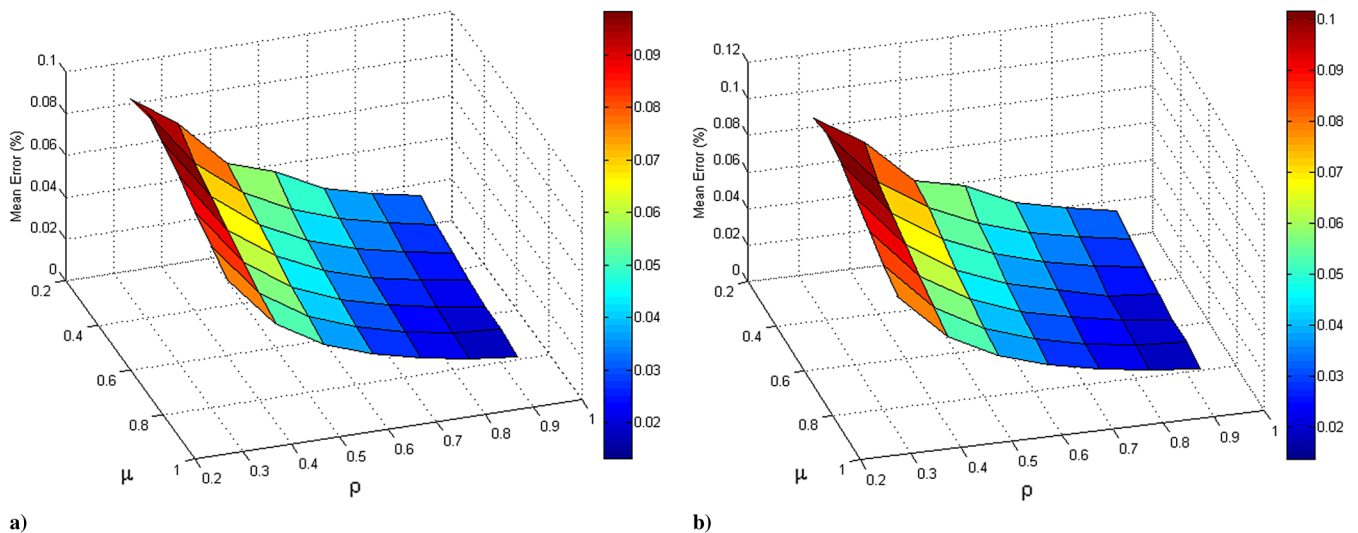
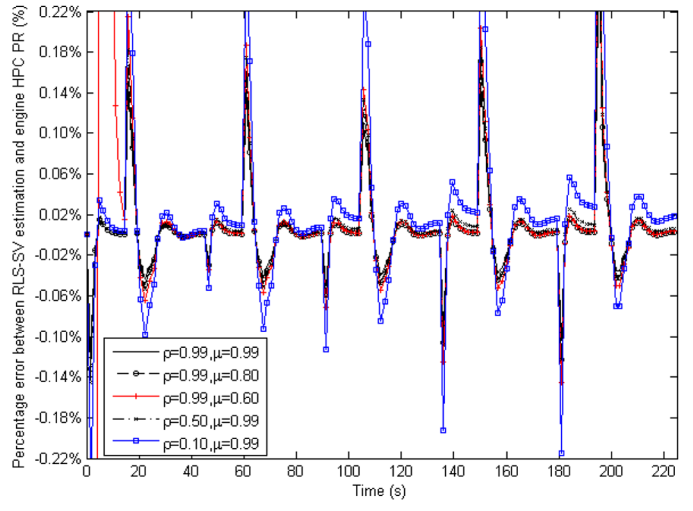
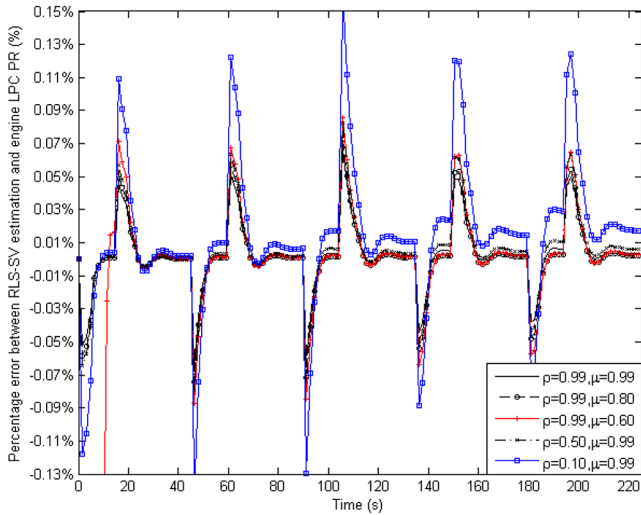


Fig. 5 Mean error to the estimation of a) LPC PR and b) HPC PR by the RLS-SI with different weights of adjustable factors.



a) **Fig. 6 Error of estimation of a) LPC PR and b) HPC PR by the RLS-SV from different weighting factors.**

$$\bar{\epsilon} = \frac{\sum_{k=0}^{225} (\hat{y}(k) - y(k)/y(k))}{k} \quad (20)$$

Unlike the RLS-SI, the adjustable term of the RLS-SV in Eq. (13) is controlled by the engine data  $\varphi$ . The change in the covariance matrix is adaptive to the gradient change of the operating line. Reducing the value of the collecting factors also reduces the adaptability and tracking capability of the RLS-SV to both compressors' pressure ratios, as shown in Fig. 6.

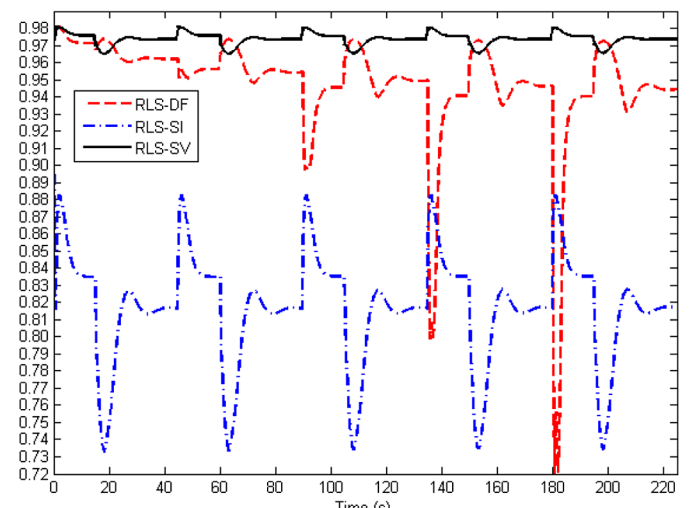
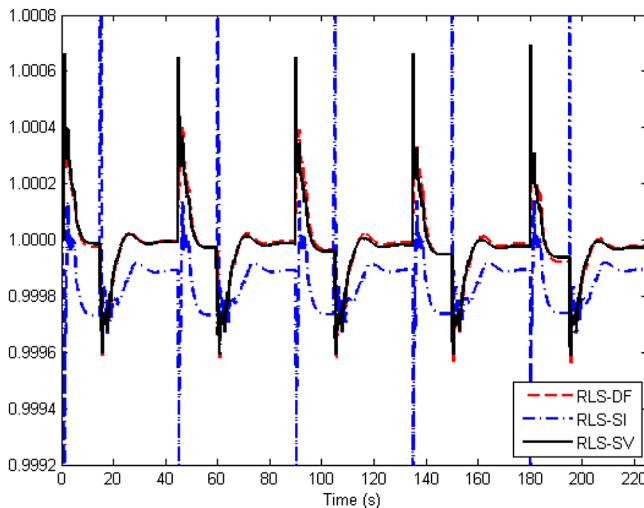
Due to the time-variant engine system, the estimated system's dynamic and stability are checked through the roots of discrete state-space functions on the  $z$  plane. For a stable system, the value of zero and the poles should be located within the unit circle on the  $z$  plane. The SS system [Eq. (19)] can be written into a second-order function with two poles and one zero. Figure 7 shows the variation of the two poles along the simulation. A linear system has a constant value of the pole and zeros. The varying routes of the SS model are caused by the engine's nonlinear dynamics and the restricted knowledge of its future response. The reliability of the identified models is important to be checked by monitoring the values of zeros and poles along the simulation. As a result, the repetitive transient operation is used to investigate the development of poles and zeros over a long time simulation. For a reliable estimation, they should be repeated for each identical transient cycle; see Fig. 7. However, the RLS-DF shows divergence on the second pole in Fig. 7b. One of the poles can exit the

unit circle when the engine is operating at a transient state; see Fig. 7a. It is because the dynamic can only be predicted according to the receding data due to the restricted knowledge of the engine future performance, and the RLS algorithms have detected the engine is operating at an unsteady region. When the operating line approaches a steady state, the value returns to the unit circle.

Figure 8 shows the values of zero for state-space model of the LPC PR and HPC PR according to Eq. (19). The locations of the zeros for both compressors are located inside the unit circle.

The stabilized RLS algorithms show effective constraints on the growth of the poles and zeros along the transient cycles; see Fig. 8. The smaller forgetting factor allows the RLS-DF to have a fast convergent speed. However, it compromises its stability; oscillations for the values of the poles or zeros are more likely to occur (Fig. 8) if the initial covariance is not accurately estimated or the transient line has a large gradient.

Decreasing the collecting factor value of the RLS-SV reduces the tracking speed as well as the stability of the estimated model. The consequence to the stability is shown by the divergence on the value of the zeros in Fig. 9. The larger value of  $\rho$  (closer to one) improves the converging speed to a stabilized zero and poles. Reducing the value of  $\mu$  affects both the covariance matrix and the adjustable term in Eq. (13) so that the pole and zeros diverge faster as the value of  $\mu$  becomes smaller; see Fig. 9. The decrease of  $\rho$  provides the impact as not much as the decrease of  $\mu$  because  $\rho$  only controls the stabilizing



a) **Fig. 7 Two poles from the discrete state-space model identified by RLS algorithms.**

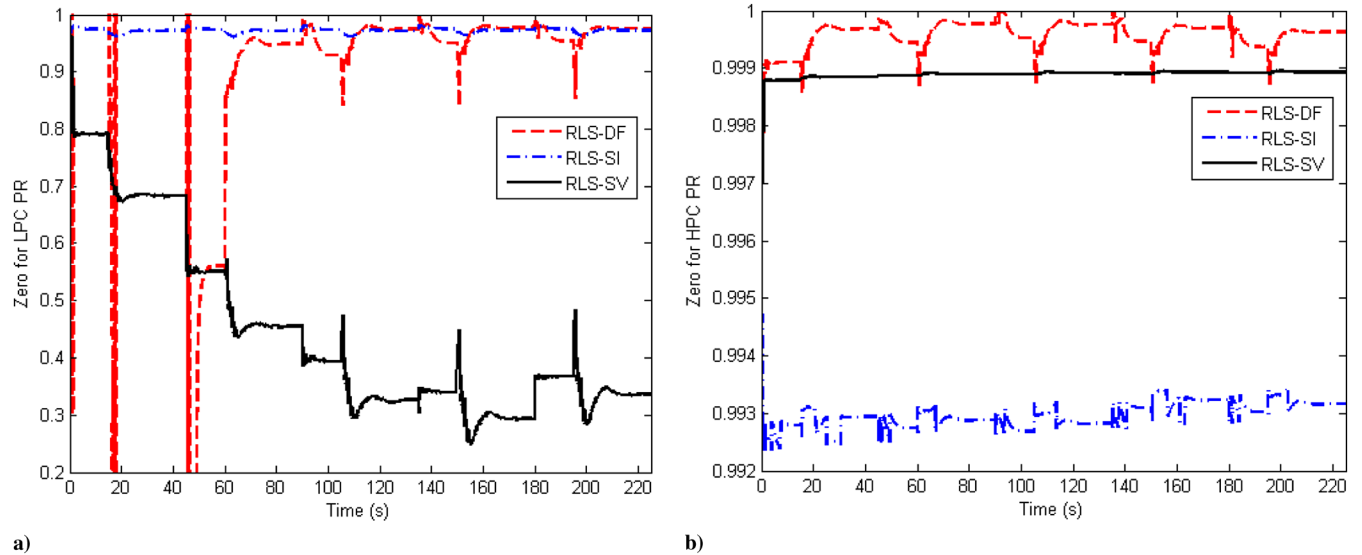


Fig. 8 Zero for state-space equation of a) LPC PR and b) HPC PR from identification of different RLS algorithms.

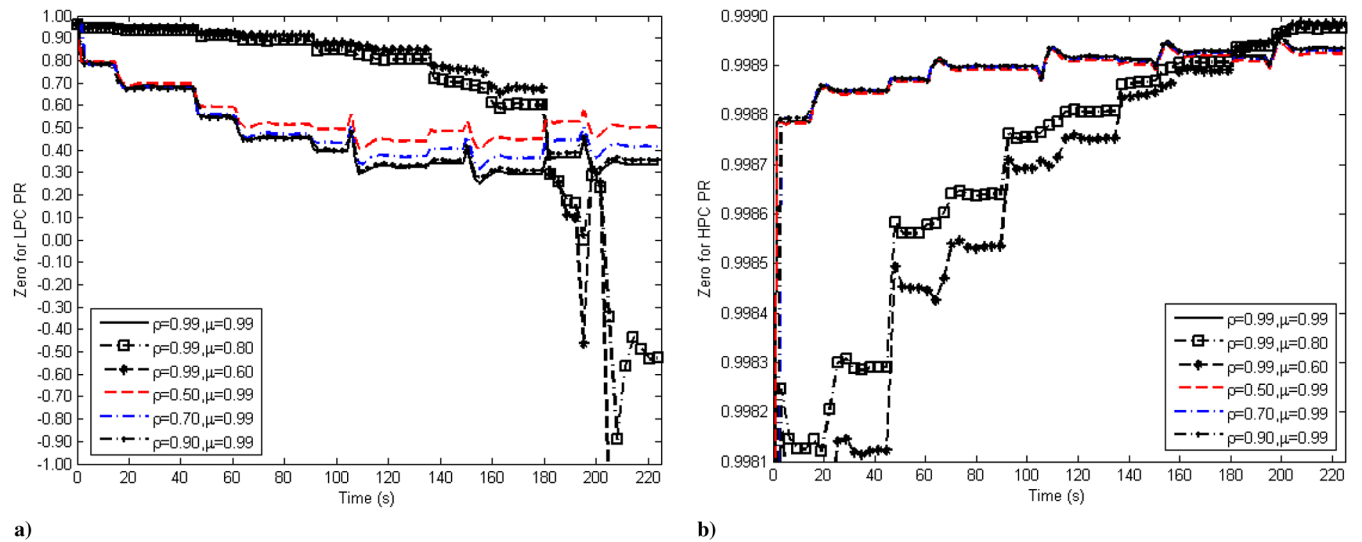


Fig. 9 Zero for state-space equation of a) LPC PR and b) HPC PR identified by the RLS-SV with different values of weight factors.

power and the influence given by the adjustable term is usually much smaller than the forgetting factor in Eq. (13) to the evolution of the covariance matrix. Therefore, in the RLS-SV,  $\mu$  controls the power to minimize the error between the estimation and engine outputs, and  $\rho$  tunes the eigenvalues to the direction of the engine state vectors within an acceptable range.

An additional investigation has been conducted on the transient operation through the entire operating range. The result of the transitions between different steady-state levels of a relative low-pressure shaft speed (0.60, 1.00, 0.95, 0.68, 0.92, 0.76, and 0.88) is shown in Fig. 10.

All RLS methods are showing an accurate estimation to the engine dynamic in Fig. 10. The stabilized RLS with the variable factor (RLS-SV) shows the smallest error of identified value to the engine LPC PR and HPC PR; see Figs. 11a and 11b. The same structure of the discrete model [Eq. (19)] can also be applied for identifying the dynamic of the relative shaft speed. The identification errors of the relative shaft speed are shown in Figs. 11c and 11d for both shafts. The variable forgetting factor from the RLS-SV allows the identified model being adaptive to the change of engine dynamics through different transient operation levels. The initial value of forgetting factors for the RLS algorithms remains the same as the previous investigation. As shown in Fig. 11, the tracking error diverges slightly if the forgetting factor is fixed in the RLS-DF or changes linearly in the RLS-SI. The value of

the forgetting factor should be tuned according to the change of transient operations in order to maintain an acceptable level of tracking accuracy.

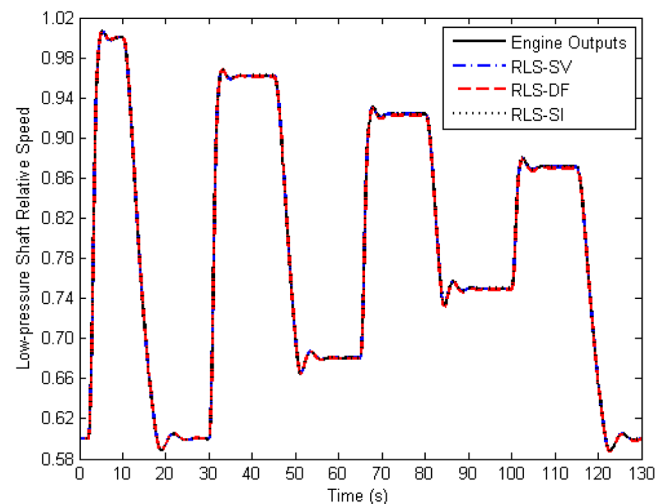
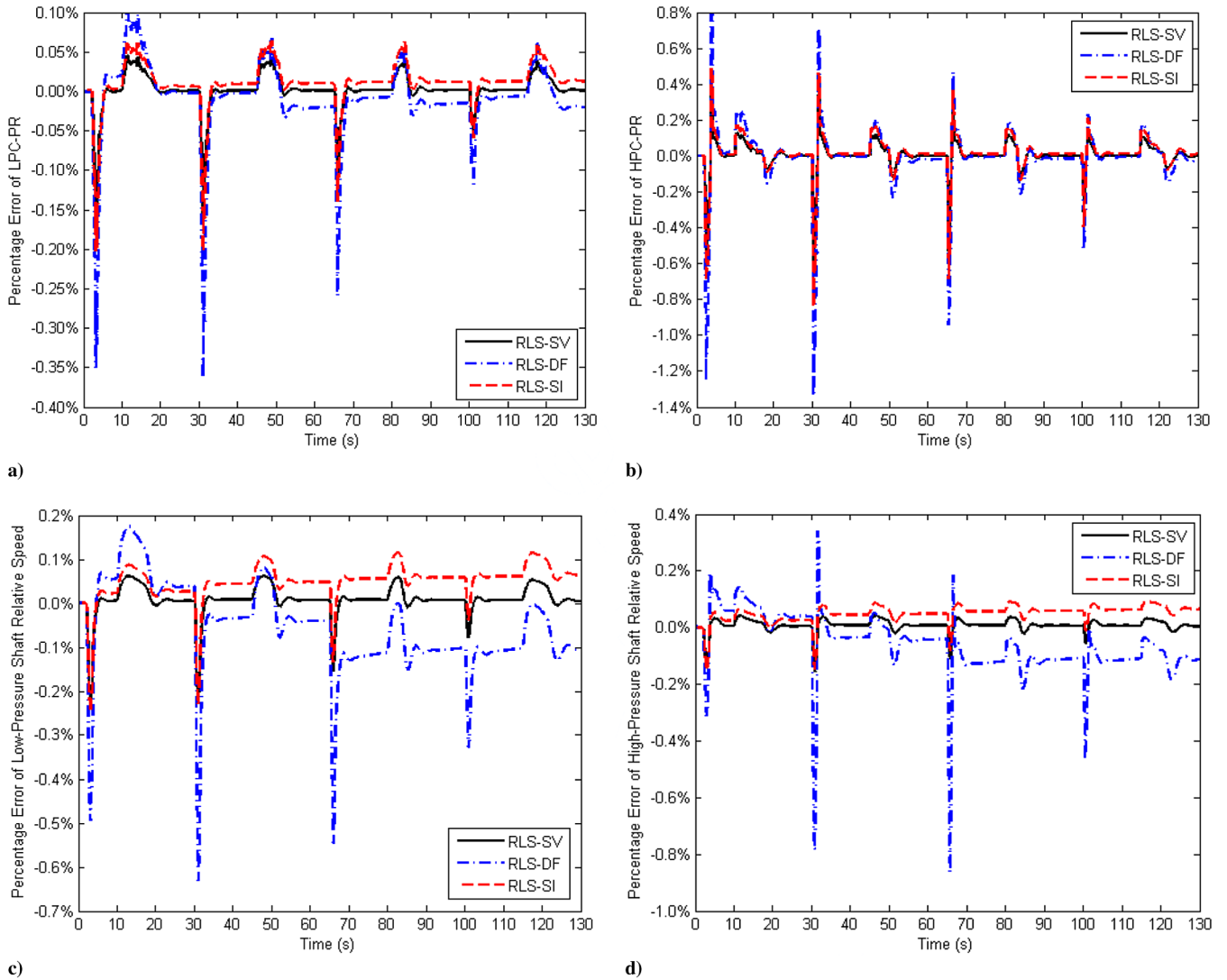


Fig. 10 Comparison of low-pressure (LP) shaft speed between the engine output and estimations.



**Fig. 11** Comparison of percentage error of the estimations from RLS algorithms to a) LPC PR, b) HPC PR, c) relative LP shaft speed, and d) relative high-pressure shaft speed.

In summary, the factor  $\mu$  in both the RLS-SI and RLS-SV performs as the forgetting factor in the RLS-DF. The adjustable term constrains the change of the covariance matrix, which can be either defined by linear factors in the RLS-SI or adjusted by the change of engine dynamic in the RLS-SV. This stabilizes the variation of the poles and zeros from the estimated model, which allows the dynamic of the estimated model to be more predictable. Furthermore, the value of the forgetting factor should be chosen so that the estimation can be compensated by the adjustable term.

## V. Conclusions

The modified recursive least-squares algorithms are applied on-line to identify the dynamic performance on a twin-spool turbofan engine. The engine is modeled to a component level. The results show that all the demonstrated RLS methods modified with forgetting factors or with adjustable terms provide good online tracking capability. The tracking accuracy is maintained over a large range of transient operations and for the transitions between different operating points.

The implementation of recursive least-squares techniques benefits the reduction of the matrix dimension from the least-squares method with an acceptable level of tracking accuracy. The directional forgetting RLS only improves the tracking accuracy from the classic RLS by shifting recursive weighting to recent data. The RLS with a constant stabilizing factor and with a varying stabilizing factor stabilizes the change of eigenvalues in the covariance matrix. Varying the  $\mu$  value, which acts as a forgetting factor, controls the power of

error minimization between the estimated model and the engine; varying the value of  $\rho$  changes the stabilizing power on the zeros and poles of the state-space model. With an adaptive weight of the stabilizing factor, the RLS-SV provides convergent tracking results over different transient operations. For the dynamic identification of gas turbine engines, the recursive length of the RLS should be adjustable in order to adapt nonlinearly dynamic change during transient operations; and the varying eigenvalues of covariance must be limited for a convergent identified model for the entire operating range.

## References

- [1] Evans, C., Fleming, P. J., Hill, D. C., Norton, J. P., Pratt, I., Rees, D., and Rodríguez-Vázquez, K., "Application of System Identification Techniques to Aircraft Gas Turbine Engines," *Control Engineering Practice*, Vol. 9, No. 2, 2001, pp. 135–148. doi:10.1016/S0967-0661(00)00091-5
- [2] Isermann, R., Baur, U., Bamberger, W., Kneppo, P., and Siebert, H., "Comparison of Six On-Line Identification and Parameter Estimation Methods," *Automatica*, Vol. 10, No. 1, 1974, pp. 81–103. doi:10.1016/0005-1098(74)90012-0
- [3] Torres, M. P., Sosa, G., Amezcua-Brooks, L., Liceaga-Castro, E., and Zambrano-Robledo, P. D. C., "Identification of the Fuel-Thrust Dynamics of a Gas Turbo Engine," *Proceedings of the IEEE Conference on Decision and Control*, IEEE, Piscataway, NJ, 2013, pp. 4535–4540. doi:10.1109/CDC.2013.6760588
- [4] Arkov, V., Evans, C., Fleming, P. J., Hill, D. C., Norton, J. P., Pratt, I., Rees, D., and Rodríguez-Vázquez, K., "System Identification Strategies

- Applied to Aircraft Gas Turbine Engines,” *Annual Reviews in Control*, Vol. 24, 2000, pp. 67–81.  
doi:10.1016/S1367-5788(00)90015-4
- [5] Paleologu, C., Benesty, J., and Ciochiña, S., “A Robust Variable Forgetting Factor Recursive Least-Squares Algorithm for System Identification,” *IEEE Signal Processing Letters*, Vol. 15, Oct. 2008, pp. 597–600.  
doi:10.1109/LSP.2008.2001559
- [6] Pilidis, P., and Maccallum, N. R. L., “A General Program for the Prediction of the Transient Performance of Gas Turbines,” *ASME International Gas Turbine Conference and Exhibit*, American Soc. of Mechanical Engineers, Fairfield, NJ, 1985, Paper V001T03A053.  
doi:10.1115/85-GT-209
- [7] Kim, S.-K., Pilidis, P., and Yin, J., *Gas Turbine Dynamic Simulation Using Simulink®*, SAE TP 2000-01-3647, Warrendale, PA, 2000,  
doi:10.4271/2000-01-3647
- [8] Bückler, D., Span, R., and Wagner, W., “Thermodynamic Property Models for Moist Air and Combustion Gases,” *Journal of Engineering for Gas Turbines and Power*, Vol. 125, No. 1, 2003, pp. 374–384.  
doi:10.1115/1.1520154
- [9] Rahman, N. U., and Whidborne, J. F., “Real-Time Transient Three Spool Turbofan Engine Simulation: A Hybrid Approach,” *Journal of Engineering for Gas Turbines and Power*, Vol. 131, No. 15, 2009, Paper 051602.  
doi:10.1115/1.3079611
- [10] Kulikov, G. G., and Thompson, H. A., “Gas Turbine Models,” *Dynamic Modelling of Gas Turbines: Identification, Simulation, Condition Monitoring and Optimal Control*, Springer Science and Business Media, New York, 2013, pp. 17–26.
- [11] Jaw, L. C., and Mattingly, J. D., “Model Reduction and Dynamic Analysis,” *Aircraft Engine Controls: Design, System Analysis, and Health Monitoring*, AIAA, Reston, VA, 2009, pp. 69–93.
- [12] Wellstead, P. E., and Zarrop, M. B., “Using Recursive Estimators,” *Self-Tuning Systems: Control and Signal Processing*, Wiley, New York, 1991, pp. 117–164.
- [13] Milek, J. J., and Kraus, F. J., “Stabilized Least Squares Estimators for Time Variant Processes,” *Proceedings of the 1st IFAC Symposium on Design Methods of Control Systems*, Vol. 2, IEEE, Piscataway, NJ, 1991, pp. 1803–1804.  
doi:10.1109/CDC.1989.70466
- [14] Milek, J. J., and Kraus, F. J., “Stabilized Least Squares Estimators: Convergence and Error Propagation Properties,” *Proceedings of the 30th IEEE Conference*, Vol. 3, IEEE, Piscataway, NJ, 1991, pp. 3086–3087.  
doi:10.1109/CDC.1991.261118
- [15] Ruano, A. E., Fleming, P. J., Teixeira, C., Rodriguez-Vázquez, K., and Fonseca, C. M., “Nonlinear Identification of Aircraft Gas-Turbine Dynamics,” *Neurocomputing*, Vol. 55, Nos. 3–4, 2003, pp. 551–579.  
doi:10.1016/S0925-2312(03)00393-X



2016-07-19

# Recursive least squares for online dynamic identification on gas turbine engines

Zhou, Li

American Institute of Aeronautics and Astronautics

---

Li Z, Nikolaidis T, Nalianda D, Recursive least squares for online dynamic identification on gas turbine engines, *Journal of Guidance, Control, and Dynamics*, Vol. 39, Issue 1, 2016, pp. 2594-2601

<https://dspace.lib.cranfield.ac.uk/handle/1826/10679>

*Downloaded from Cranfield Library Services E-Repository*